PROCEEDINGS OF SCIENCE

A Numerical Study of Cosmic-Ray Nuclei and Isotope Propagation

Zachary Dorris,[a,*] **Yuca Chen,**[a] **Vladimir S. Ptuskin**[b] **and Eun-Suk Seo**[a,b]

[a] *University of Maryland, College Park, Department of Physics, 4150 Campus Dr, College Park, MD 20740*

[b] *Institute of Physical Science & Technology, 4254 Stadium Dr, College Park, MD 20740*

E-mail: zdorris@umd.edu, ychen150@terpmail.umd.edu, vptuskin@hotmail.com, seo@umd.edu

Recent high-precision measurements of various types of particles in cosmic rays provide an unprecedented opportunity to study the structure of the galaxy. Radioactive cosmic-ray secondaries, such as beryllium-10 or aluminium-26, decay during propagation on a similar time scale to their escape time from the galaxy. As a result, the isotopic composition of these cosmic rays provides information about propagation time scales. We examined the energy dependence of cosmic-ray spectra and isotopic compositions, with a particular focus on the isotopes of beryllium. These data were considered in the context of a plain diffusion model with reacceleration effects, using a propagation code, GALPROP, to compute predicted elemental and isotopic spectra. The implications of the data on transport and source parameters in this model will be discussed. The impact of nuclear cross section uncertainties on these parameters will also be examined.

38th International Cosmic Ray Conference (ICRC2023)
26 July - 3 August, 2023
Nagoya, Japan

*Speaker

PoS(ICRC2023)070

1. Introduction

It is known that certain unstable radioactive nuclei found in cosmic rays can be used to constrain the age of cosmic rays [1]. In particular, nuclei with lifetimes similar in magnitude to their escape time from the galaxy - known as radioactive clocks - allow us to infer their age by measuring their abundance compared to stable counterpart nuclei. The $^{10}Be/^{9}Be$ ratio is a particularly well-measured example of such a ratio, with precision measurements being provided by several experiments in recent years [2, 3, *and references therein*]. These precision measurements make for an excellent opportunity to study the properties of cosmic-ray propagation, especially those related to the time scale of cosmic-ray escape.

These studies are complicated by the need to understand both the relative production rates of these nuclei in the interstellar medium, connected to their nuclear cross-sections, as well as the need to understand how cosmic rays propagate through the galaxy, connected to the structure of the galaxy and the properties of the ISM. To better understand the effect of these complications, various models of CR propagation have been developed both numerically and analytically. These models help to clarify the effect of various propagation effects, such as diffusion, reacceleration, energy loss, and fragmentation on measured fluxes at Earth. However, the validity of calculations from these models remains dependent on the precision with which the network of nuclear production cross sections is known. In this work, we investigate the effect of current uncertainties in nuclear production rates on the determination of transport parameters using numerical propagation codes. These uncertainties are further used to provide statistical constraints on the value of the halo size of the galaxy.

2. Methods

In order to study propagation effects on cosmic rays, version 57 of the propagation code GALPROP was used [4]. GALPROP numerically solves the transport equation, a particular system of governing equations for cosmic-ray flux which includes terms for diffusion effects, source injection, reacceleration and energy loss, and decay and fragmentation. This set of equations includes one equation for every species of cosmic ray under consideration, and these are solved as a network in order to facilitate the inclusion of radioactive decay and fragmentation. The free parameters of the model were tuned to experimental data via MINUIT2, an external optimization package which uses robust variants of the gradient descent algorithm to find parameters that minimize a specified function [5]. The effects of solar modulation are also included via the well-known force-field approximation [6], with the modulation potential ϕ left as a free parameter.

Within GALPROP, the spatial diffusion coefficient is modeled as a broken power law in rigidity, following the form $D_{xx} \propto \beta(R)^{\delta}$ where δ can be constant or can change its value at specified break rigidities. This work uses a constant value of δ at all rigidities. The value of D_{xx} at the reference rigidity 4 GV is given by the parameter D_0. The source injection spectra of primary nuclei similarly follow broken power laws in rigidity of the form $q \propto R^{-\gamma}$, with γ changing its value above and below a break set at 9 GV. The exact relation depends on the source abundance of the isotope in question.

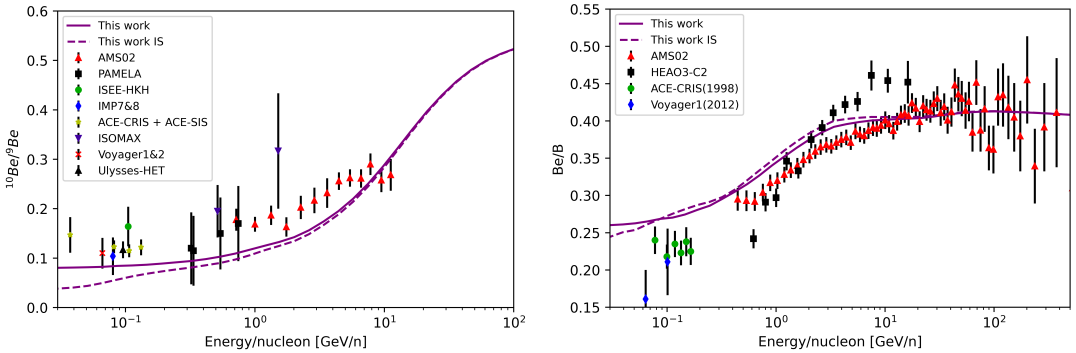

Figure 1: The cosmic-ray $^{10}Be/^{9}Be$ ratio (left) and the Be/B ratio (right) as functions of kinetic energy per nucleon. The points represent data with error bars, while the lines represent models calculated using our parameter values in GALPROP. The dashed lines are interstellar spectra, while the solid lines are modulated using a potential of $\phi = 407$ MV. Data references for the $^{10}Be/^{9}Be$ ratio are given in [2, 3, 8–13], and for the Be/B ratio by [14–17]

The galaxy is modeled as cylindrically shaped, with a halo size H denoting the half-width of the diffusive region. The ratios of secondary nuclei to primary nuclei, such as the boron-to-carbon ratio, are known to be roughly proportional to D_{xx}/H in this model [7]. The under-determination of these parameters can be solved by including unstable-to-stable ratio data, permitting separate determination of the model parameters D_0 and H.

Optimization of parameters using the MINUIT2 package requires both the declaration of which model parameters should be optimized, as well as a set of experimental data against which predicted spectra will be compared. In order to prevent loss of accuracy from conflicting data sets, the experimental data used for MINUIT optimization included only data from the AMS02 instrument and the ACE-CRIS instrument, as well as interstellar data gathered by the instruments onboard Voyager1 in 2012. The spectra for Be, B, C, O, Mg, and Si were included in the target data set, as well as measurements of the B/C ratio, the Be/B ratio, and the $^{10}Be/^{9}Be$ ratio. The C, O, Mg, and Si spectra were chosen as they represent the most abundant primaries that can fragment and produce isotopes of beryllium; the Be, B, and B/C spectra were chosen to represent two important secondaries, and to further constrain diffusion parameters; and the Be/B and $^{10}Be/^{9}Be$ ratios were chosen to break the degeneracy of D_0 and H.

3. Results and Discussion

Following optimization, various cosmic-ray spectra were computed in GALPROP using the values found by MINUIT2. For the diffusion parameters, we used a value of $\delta = 0.396$ and a value of $D_0 = 9.47\ x\ 10^{28}\ cm^2 s^{-1}$. The source injection slope was $\gamma = 1.76$ and $\gamma = 2.43$ below and above the 9 GV break, respectively. Reacceleration effects were included using an Alfvén velocity of 29 km/s. The value of the halo size used for this initial calculation was 11.3 kpc, with a fitting uncertainty of 0.21 kpc.

Figure 1 shows measurements of the $^{10}Be/^{9}Be$ ratio, as well as the Be/B ratio, plotted along with predicted spectra computed using the values above. These two ratios are particularly sensitive

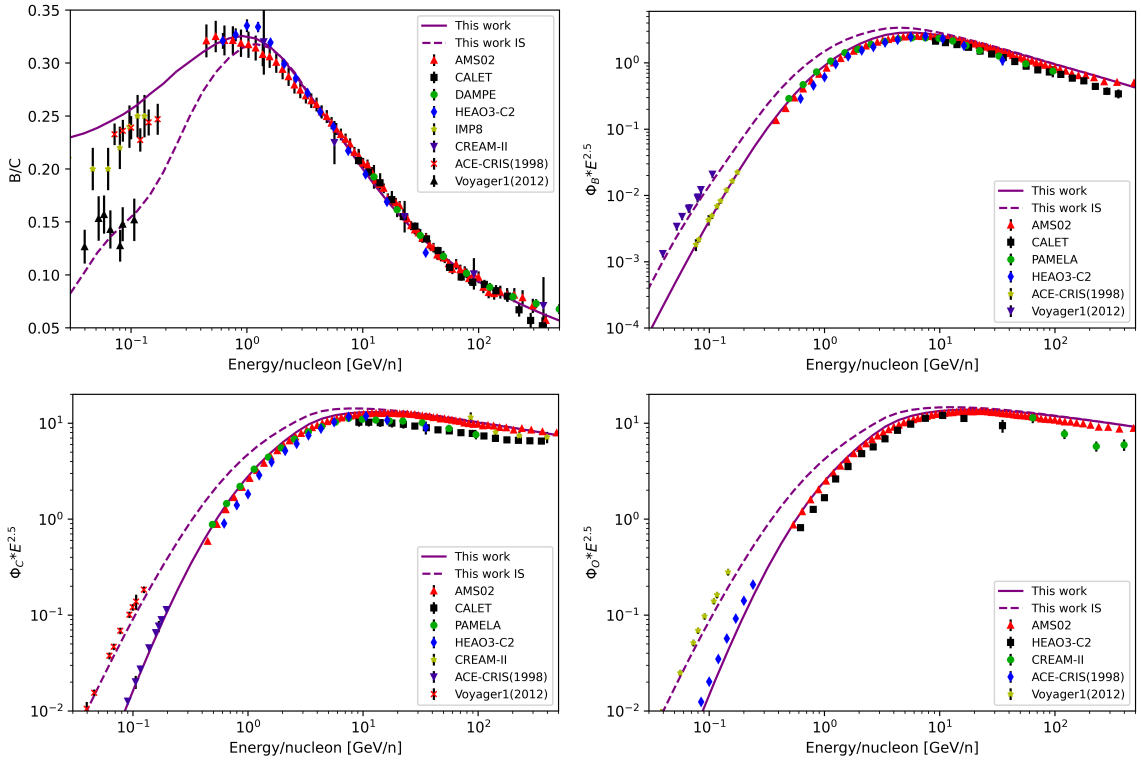

Figure 2: Several cosmic-ray spectra computed using the GALPROP framework, plotted alongside experimental data. The meaning of the lines and points is the same as in figure 1. (top left) The boron-to-carbon ratio [14–21]. (top right) The boron spectrum [14–17, 20, 22]. (bottom left) The carbon spectrum [14–17, 20, 22, 23]. (bottom right) The oxygen spectrum [14–17, 23].

to the choice of halo size, as the $^{10}Be \longrightarrow {}^{10}B$ decay chain produces an effect in both the numerator and denominator of these ratios. Thus, the halo size is greatly constrained by these data.

Figure 2 shows several other cosmic-ray spectra, computed in the same manner. These spectra are useful to set the ratio D_0/H, permitting the determination of H from radioactive clock data. It is also important that the main progenitors of beryllium, namely boron, nitrogen, and the primary elements up to silicon, are fit well. This allows for the calculation of the secondary beryllium spectrum to be as self-consistent as possible with other cosmic-ray data. It is notable that, even with these progenitors fit well, these calculations still shows an excess below about 10 GeV/n in the Be/B ratio. This excess is a persistent feature in the beryllium spectrum specifically, as other secondary species like boron are fit well.

To quantify the effect of nuclear uncertainties on the values of H found above, we examine the database of experimental nuclear cross-section measurements for various production channels from GALPROP's internal nuclear package, specifically the file *isotope_cs.dat*. The data was filtered to data points at or above 500 MeV/nucleon, as this is the most relevant energy range for our study, and constant functions were fit to the data for each of the beryllium-producing channels present in the file. The choice of a constant function comes from the form of the most common fitting function to cross-section data, which is a constant plus an exponentially decaying sine function to account for nuclear resonances. For the production channels discussed here, the exponentially-decaying

Channel	Fit σ (mb)	95% CI (mb)
$^{12}C \longrightarrow {}^{9}Be$	5.72	[5.16, 6.28]
$^{12}C \longrightarrow {}^{10}Be$	3.40	[3.02, 3.78]
$^{16}O \longrightarrow {}^{9}Be$	3.80	[3.10, 4.50]
$^{16}O \longrightarrow {}^{10}Be$	1.65	[1.43, 1.87]
$^{14}N \longrightarrow {}^{9}Be$	2.00	[0.80, 3.20]
$^{14}N \longrightarrow {}^{10}Be$	1.48	[0.74, 2.22]

Table 1: Constant cross-sections fit to the most impactful production channels of ^{9}Be and ^{10}Be in cosmic rays, along with 95% confidence intervals on these constant fits. Fits are performed to data found in GALPROP's internal nuclear package, and only at energies above 500 MeV/nucleon.

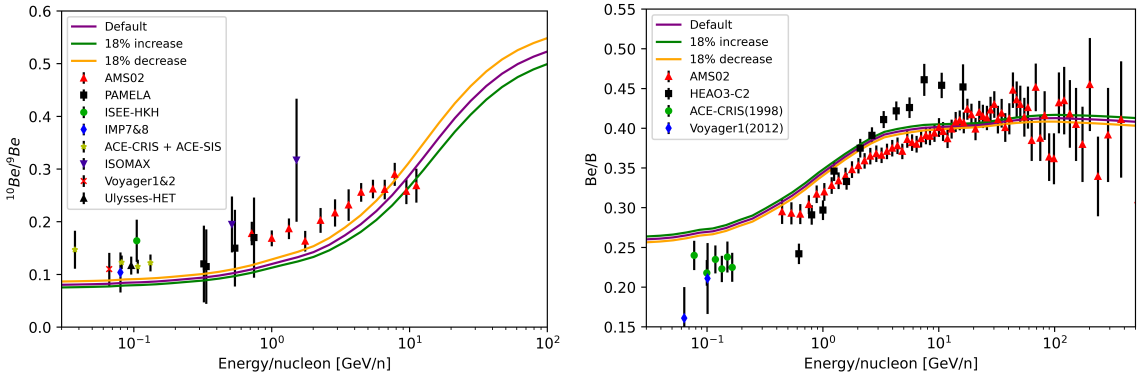

Figure 3: Several predicted curves for the $^{10}Be/^{9}Be$ ratio and the Be/B ratio, each computed using a different value for the cross-section of the $^{16}O \longrightarrow {}^{9}Be$ production channel. The curves show the effect of altering this production cross-section by a constant factor within the constraints of the 95% confidence interval calculated previously.

portion mostly dominates at lower energies than 500 MeV/nucleon, so we can reasonably fit only the constant part of the fitting function. 95% confidence intervals were also constructed for the constants for each channel. The results of these fits are summarized in table 1.

Figure 3 shows the halo-size-sensitive measurements shown in figure 1, but with the halo size and diffusion parameters re-optimized using alternative production cross-sections. The production cross-section of the $^{16}O \longrightarrow {}^{9}Be$ channel is varied by a constant factor, from a uniform 18% decrease in cross-section to a uniform 18% increase. The choice of 18% is made in order to remain just within the bounds of the 95% confidence interval on this channel found previously. We used a halo size of 9.0 kpc for the calculation with an 18% decrease in cross-section, and 15.0 kpc for the calculation with an 18% increase in cross-section, both found using MINUIT2 as previously described.

The variation in both the computed spectra and the calculated H value shows that the effects of nuclear uncertainties, even within general consistency with experimental nuclear data, are not insignificant in the determination of transport parameters in the diffusive model of cosmic-ray propagation. The $^{16}O \longrightarrow {}^{9}Be$ reaction is shown here as a particularly extreme example of this; the high abundance of oxygen in cosmic rays combined with the low precision of existing measurements,

as shown in table 1, makes this reaction very impactful on GALPROP's results. We find that, within nuclear uncertainties, the halo size can range at least from 9.0 kpc to 15.0 kpc. This range shows vastly more uncertainty compared to the 11.3 ± 0.2 kpc value found from the original MINUIT2 fit using default cross-sections. It's clear that precise determination of transport parameters, especially from data concerning isotopic abundances in cosmic rays, is highly dependent on knowledge of the cross-sections involved in the nuclear network.

4. Conclusions

We used the GALPROP framework, along with MINUIT2's optimization capabilities, to place constraints on the diffusive halo size of the galaxy in light of recent measurements of the $^{10}Be/^{9}Be$ and Be/B ratios in cosmic rays. We found that using the default cross-sections in GALPROP, the halo size is calculated to be 11.3 ± 0.2 kpc. Various other transport and source parameters were optimized in parallel to the halo size, providing a self-consistent model for several relevant elemental spectra.

We further considered the impact that nuclear cross-section uncertainties could have in lowering our confidence in the value of the halo size. We used constant fits to estimate the variance in cross-sections permitted while remaining consistent with experimental data. We then used these variances to compute the impact of the particularly poorly-measured $^{16}O \longrightarrow {}^{9}Be$ decay chain's uncertainties in the halo size determination. We found that, within nuclear uncertainties, the halo size is constrained at best to the range [9.0, 15.0] kpc, significantly wider than the fitting uncertainty of the procedure. These findings emphasize the importance of having precise measurements of the nuclear network cross-sections in studying the propagation of cosmic rays.

References

[1] S. Hayakawa, K. Ito, and Y. Terashima, *"Origin of Cosmic Rays"*, PTPS **6** (1958)

[2] F. Dimiccoli, *Cosmic-Ray Beryllium Isotopes with AMS02*, *ECRS 2022*, Proceedings of Science, 2022. PoS(ECRS)068

[3] F. Nozzoli and C. Cernetti *"Beryllium Radioactive Isotopes as a Probe to Measure the Residence Time of Cosmic Rays in the Galaxy and Halo Thickness: A "Data-Driven" Approach"*, Univ **7** (2021)

[4] T. Porter, G. Jóhannesson, and I. Moskalenko, *"The GALPROP Cosmic-ray Propagation and Nonthermal Emissions Framework: Release v57"*, ApJS **262** (2022) https://galprop.stanford.edu/

[5] F. James and M. Roos, *"Minuit - a system for function minimization and analysis of the parameter errors and correlations"* Comput. Phys. Commun. **10**, (1975)

[6] L. Gleeson and W. Axford, *"SOLAR MODULATION OF GALACTIC COSMIC RAYS"*, ApJ **154** (1968)

[7] T. Gaisser, R. Engel, and E. Resconi, *Cosmic Rays and Particle Physics 2nd ed.*, Cambridge University Press, 2016

[8] A. Lukasiak et. al., *"The Isotopic Composition of Cosmic-Ray Beryllium and Its Implication for the Cosmic Ray's Age"*, ApJ **423** (1994)

[9] J. J. Connell, *"Galactic Cosmic-Ray Confinement Time: Ulysses High Energy Telescope Measurements of the Secondary Radionuclide ^{10}Be"*, ApJ **501** (1998)

[10] T. Hams et. al., *"Measurement of the Abundance of Radioactive ^{10}Be and Other Light Isotopes in Cosmic Radiation up to 2 GeV Nucleon^{-1} with the Balloon-borne Instrument ISOMAX"*, ApJ **611** (2004)

[11] M. E. Wiedenbeck. and D. E. Greiner, *"A cosmic-ray age based on the abundance of Be-10"*, ApJ **239** (1980)

[12] M. Garcia-Munoz, G. M. Mason, and J. A. Simpson, *"The age of the galactic cosmic rays derived from the abundance of ^{10}Be"*, ApJ **217** (1977)

[13] N. E. Yanasak et. al., *"Measurement of the Secondary Radionuclides ^{10}Be, ^{26}Al, ^{36}Cl, ^{54}Mn, and ^{14}C and Implications for the Galactic Cosmic-Ray Age"*, ApJ **563** (2001)

[14] M. Aguilar et. al., *"The Alpha Magnetic Spectrometer (AMS) on the international space station: Part II - Results from the first seven years"*, PhR **894** (2021)

[15] A. C. Cummings et. al., *"Galactic Cosmic Rays in the Local Interstellar Medium: Voyager 1 Observations and Model Results"*, ApJ **831** (2016)

[16] K. A. Lave et. al., *"Galactic Cosmic-Ray Energy Spectra and Composition during the 2009-2010 Solar Minimum Period"*, ApJ **770** (2013)

[17] J. J. Engelmann et. al., *"Charge composition and energy spectra of cosmic-ray nuclei for elements from Be to Ni - Results from HEAO-3-C2"*, A&A **223** (1990)

[18] H. S. Ahn et. al., *"Measurements of cosmic-ray secondary nuclei at high energies with the first flight of the CREAM balloon-borne experiment"*, APh **30** (2008)

[19] DAMPE Collaboration, *"Detection of spectral hardenings in cosmic-ray boron-to-carbon and boron-to-oxygen flux ratios with DAMPE"*, SciBu **67** (2022)

[20] O. Adriani et. al., *"Cosmic-Ray Boron Flux Measured from 8.4 GeV /n to 3.8 TeV /n with the Calorimetric Electron Telescope on the International Space Station"*, PhRvL **129** (2022)

[21] M. Garcia Munoz et. al., *"Cosmic-Ray Propagation in the Galaxy and in the Heliosphere: The Path Length Distribution at Low Energy"*, ApJS **64** (1987)

[22] O. Adriani et. al., *"Measurement of Boron and Carbon Fluxes in Cosmic Rays with the PAMELA Experiment"*, ApJ **791** (2014)

[23] H. S. Ahn et. al., *"Energy Spectra of Cosmic-ray Nuclei at High Energies"*, ApJ **707** (2009)